Chapter 4

Metamaterial Properties of 2D Ferromagnetic Nanostructures: From Continuous Ferromagnetic Films to Magnonic Crystals

Roberto Zivieri

Additional information is available at the end of the chapter

http://dx.doi.org/10.5772/64070

Abstract

In recent years the study of low-dimensional magnetic systems has become topical not only for its several technological applications but also for achieving a deep understanding of the underlying physics of magnetic nanostructures. These efforts have considerably advanced the field of magnetism both theoretically and from an experimental point of view. Very recently, for their challenging features, great attention has been given to the investigation of the static and dynamical properties of magnetic nanostructures with special regard to magnonic crystals, a class of periodic magnetic systems. As shown by micromagnetic and analytical methods, the ferromagnetic materials composing magnonic crystals can be regarded as metamaterials since they exhibit effective properties directly linked, for instance, to the definition of an effective magnetization, an effective permeability, and an effective wavelength. Hence, the aim of this chapter is to give an overview of the recent results obtained on the study of metamaterial properties of two-dimensional ferromagnetic nanostructures ranging from those of thin films to the ones of two-dimensional magnonic crystals. Some possible applications based on the effective properties for tailoring new magnetic devices are suggested.

Keywords: metamaterials, ferromagnetic nanostructures, magnonic crystals, effective properties, magnonic devices

1. Introduction

In this chapter, an overview of recent theoretical results on metamaterial properties of ferromagnetic nanostructures is presented. These results have been found according to micromag-

netic simulations based on a finite difference method called dynamical matrix method (DMM) with implemented two-dimensional (2D) boundary conditions and extended to periodic magnetic systems [1] and via simple analytical calculations. We first review some challenging properties arising from the study of spin dynamics in in-plane magnetized ferromagnetic thin films that can be regarded as the simplest example of ferromagnetic nanostructures. Indeed, they are un-patterned and infinitely extended systems in the *xy* plane but are confined along the *z* direction with thickness of a few nanometers. There are several studies carried out on spin-wave modes propagation in ferromagnetic films with both in-plane and out-of-plane magnetization and different classes of excitations based on the propagation features have been studied (see e.g., [2, 3]). Special emphasis is devoted to the investigation of backward volume spin-wave modes (BVMSWs) characterized by a "negative" group velocity (antiparallel to the propagation wave vector) and a negative dynamic permeability in the magnetostatic limit (see e.g., [3, 5]). This analysis is done for the sake of simplicity in the absence of losses but it can be easily generalized also to spin dynamics where intrinsic damping is taken into account. It is shown that the inclusion of the exchange interaction suppresses the backward nature of BVMSWs leading to a "positive" group velocity, namely a group velocity parallel to the propagation wave vector, and the analytical expressions of the group velocity are given in both the dipole and dipole-exchange regimes [4]. Moreover, it is demonstrated that BVMSWs are spin-wave modes characterized by a negative dynamic effective permeability and its behavior is studied as a function of the spin-wave mode frequency and magnetic parameters [5]. In view of these results, ferromagnetic thin films with in-plane magnetization can be regarded as metamaterials and can be put on a similar footing as other classes of metamaterials such as electromagnetic backward-wave media where, since the first prediction by Veselago [6], the simultaneous presence of a negative permeability and permittivity was investigated (see e.g., [7, 8]).

Then, the analysis focuses on periodic two-dimensional (2D) magnetic nanostructures with periodic modulation, the so-called magnonic crystals (MCs) [9–17], by giving special emphasis to their metamaterial properties arising from the 2D spatial periodicity. Specifically, effective quantities such as the notions of effective magnetization, effective wavelength, and effective wave vector are introduced for different kinds of 2D magnonic crystals. In particular, these properties are discussed for square arrays of antidot lattices (ADLs) where holes are embedded into a ferromagnetic matrix (single component systems) and binary systems composed by periodic arrangements of dots etched into a ferromagnetic matrix of a different material. General relations involving the effective wavelength and effective wave vector with the corresponding Bloch wavelength and Bloch wave vector are proposed for in-plane [17] and perpendicularly magnetized ADLs [18], and it is shown that their validity can be extended to periodic and binary systems [19, 20]. An effective relation involving the effective wave vector and completing the well-known Bloch rule for periodic systems is also presented. Frequency dispersion and band gaps of collective modes are discussed for different geometries and comparisons with the frequencies calculated via an effective description are performed. The definition of effective "surface magnetic charges" is introduced for describing the magnetic interactions in binary ferromagnetic systems in terms of an effective magnetic potential and experiment for tailoring magnetic devices and for mapping the spatial profiles of collective spin-wave modes based on the studied effective properties is proposed [17].

http://dx.doi.org/10.5772/64070

2. Metamaterial properties of ferromagnetic films

In this section, we review the metamaterial properties of ferromagnetic thin films that can be considered as the simplest example of ferromagnetic nanostructures. In particular, we focus on some recent theoretical results on the dynamical properties related to a class of volume spin-wave modes whose wave vector is parallel to the static magnetization **M** and to the external magnetic field **H**, sometimes called BVMSW. These modes are characterized by a "negative" group velocity $\mathbf{v}_g$ [4]. The word "negative" refers to the fact that, for this class of spin-wave modes, the group velocity is opposite to the propagation wave vector **k** and to the phase velocity. As a result, BVMSW frequency decreases with increasing the modulus of the propagating wave vector. This unusual behavior is associated to their propagation that is along the direction of the in-plane magnetic field and of the magnetization leading to a reduction of their magnetostatic energy with increasing the modulus of the wave vector.

2.1. BVMSWs and group velocity

BVMSWs are thermally excited waves typical of the in-plane magnetized ferromagnetic thin film depicted in **Figure 1**, having the following features:

1. They are classified as volume spin waves because they have a real perpendicular to the plane wave vector component.
2. They are characterized by a "negative" group velocity satisfying the condition $\mathbf{k}\cdot\mathbf{v}_g < 0$ according to which the group velocity $\mathbf{v}_g = (0, v_g)$ is antiparallel to the in-plane wave vector $\mathbf{k} = (0, k_y)$ and to the phase velocity.
3. They are transverse plane waves, that is $\mathbf{k}\cdot\delta\boldsymbol{m} = 0$ with $\delta\boldsymbol{m}(\mathbf{x}) = \delta\boldsymbol{m}_0 \exp^{i(\mathbf{k}\cdot\mathbf{x}-\omega t)}$ where $\delta\boldsymbol{m} = (\delta m_x, \delta m_z)$ is the dynamic magnetization, $\delta\boldsymbol{m}_0 = (\delta m_{0x}, \delta m_{0z})$ is the dynamic magnetization amplitude with $\mathbf{x} = (x, y)$ for **M** and **H** oriented along the y axis. The corresponding band of frequencies lies below that of the surface waves, the so-called Damon-Eshbach modes.

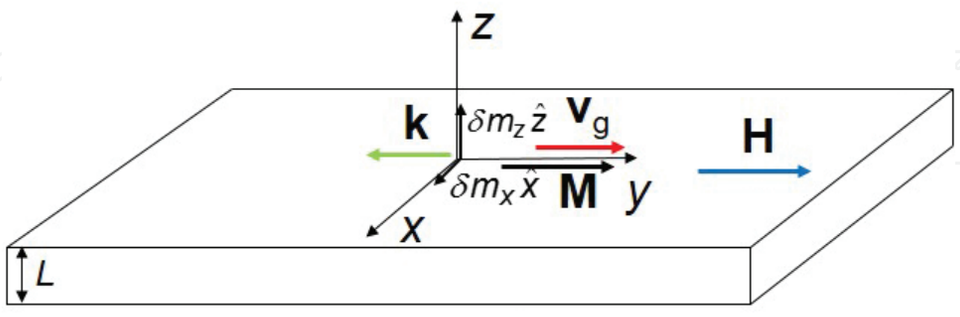

Figure 1. Sketch of the ferromagnetic film. The directions of **H**, **M**, **k**, and $\mathbf{v}_g$ of BVMSW are shown. The dynamic magnetization components δm_x and δm_z are also indicated. The symbol L denotes the thickness.

Note that in ferromagnetic thin films, there exists also volume modes having $\mathbf{k} = (k_x, k_y)$ even though they cannot be classified, at all effects, as BVMSWs that have a propagating wave vector along the direction of **M** and **H**.

The spectrum of BVMSWs in dimensionless units in the dipole-exchange regime for a purely conservative dynamics (no Gilbert damping) and assuming the dynamic magnetization uniform along z takes the form [3]:

$$\Omega_k^2 = \left(\Omega_{\text{Heff}} + \Omega_{\text{Hexch}}\right)\left(\Omega_{\text{Heff}} + \Omega_{\text{Hexch}} + \frac{1 - e^{-kL}}{kL}\right). \tag{1}$$

where $\Omega_k = \omega/\omega_M$ with ω the angular frequency and $k = |k_y|$, $\omega_M = 4\pi\gamma M$ with γ the gyromagnetic ratio (in modulus) and M the saturation magnetization, $\Omega_{\text{Heff}} = H_{\text{eff}}/4\pi M$ and $\Omega_{\text{Hexch}} = H_{\text{exch}}/4\pi M$. H_{eff} is the effective field including in this case the external magnetic field H only, namely $H_{\text{eff}} = H$ and $\Omega_{\text{Heff}} = \Omega_H$ being the demagnetizing field for in-plane magnetization equal to zero and, for the sake of simplicity, within this description the anisotropy is neglected, $H_{\text{exch}} = Dk^2$ (D is the exchange constant) is the dynamic non-uniform exchange field. The term effective field is used in this framework to underline the metamaterial and effective properties characterizing this family of spin waves such as the "negative" group velocity or the negative permeability depending on H_{eff}. Strictly speaking, the purely magnetostatic regime occurring when $H_{\text{exch}} = 0$ corresponds to angular frequencies in the microwave range and wave vectors between 30 and 10^5 cm^{-1} where electromagnetic retardation effects are neglected. In this regime, in the limit of infinite wave vector, the angular frequency is the Larmor resonance frequency, viz. $\omega = \gamma H_{\text{eff}}$ that becomes $\omega = \gamma H$ when anisotropy is not included. In a realistic calculation also exchange effects should be taken into account for wave vectors larger than 10^5 cm^{-1}. From Eq. (1), the group velocity $\mathbf{v}_g = \nabla_{\mathbf{k}}\omega$, where $\nabla_{\mathbf{k}}$ denotes the gradient with respect to the wave vector can be calculated. For the geometry shown in **Figure 1**, it is $\mathbf{v}_g = (0, v_g)$ with $v_g = \partial\omega/\partial k$. In the magnetostatic limit, we get:

$$\mathrm{v}_g = -\frac{\omega_M}{2}\frac{\Omega_{\text{Heff}}}{\Omega_k}\frac{1}{k}\frac{1 - e^{-kL}(1 + kL)}{kL}, \tag{2}$$

with $v_g < 0$. The behavior of the group velocity given in Eq. (2) as a function of the modulus of the in-plane wave vector is illustrated in **Figure 2** for $L = 10$ nm and for two different values of the effective field, $\Omega_{\text{Heff}} = 0.1$ and $\Omega_{\text{Heff}} = 1$, respectively. In the calculations, typical parameters of ferromagnetic materials were used: $\gamma = 1.76 \times 10^7$ rad/(G s), $4\pi M = 10^4$ G, and $D = 0$. The group velocity is of the order of hundreds of meters per second, has its minimum value in the long wavelength limit ($k = 0$), increases with increasing k tending asymptotically to zero (negatively) for large wave vectors in proximity of the Larmor resonance frequency. At fixed magnetic parameters, the group velocity increases (negatively) with increasing the thickness L of the ferromagnetic film.

http://dx.doi.org/10.5772/64070

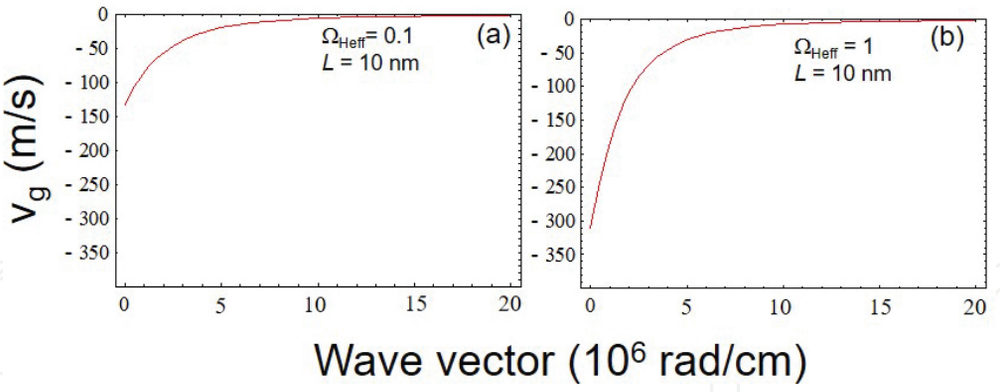

Figure 2. Group velocity v_g of BVMSWs as a function of the in-plane wave vector in the magnetostatic limit for L = 10 nm. (a) v_g for Ω_{Heff} = 0.1. (b) v_g for Ω_{Heff} = 1.

In the presence of exchange effects, BVMSWs propagation is studied in the dipole-exchange regime. From Eq. (1), we get the corresponding group velocity that depends also on the exchange field, namely:

$$v_g = \frac{\omega_M}{2}\frac{1}{\Omega_k}\frac{1}{k}\frac{\left(4\Omega_{H_{exch}}^2 + 4\Omega_{Heff}\Omega_{H_{exch}} + \Omega_{H_{exch}}e^{-kL} + \Omega_{Heff}e^{-kL}\right)kL + \left(\Omega_{H_{exch}} - \Omega_{Heff}\right)\left(1 - e^{-kL}\right)}{kL} \tag{3}$$

Group velocity is still "negative" for small values of the wave vector, but this behavior is suppressed by the presence of exchange effects. Above a certain value of the wave vector, group velocity becomes parallel to the phase velocity due to the effect of $H_{exch} = Dk^2$. For a given $k = k^*$, depending on the geometric and magnetic parameters and in the range of $10^4 \div 10^5$ rad/cm, it is $v_g(k^*) = 0$ for a typical exchange constant $D = 2.51 \times 10^{-9}$ Oe cm^2. For $k = k^*$, the envelope of the wave form stops as a consequence of the vanishing of the group velocity, while the corresponding phase velocity remains different from zero. For wave vectors larger than k^*, the backward nature of these volume waves is suppressed.

2.2. BVMSWs and effective permeability studied in the magnetostatic approximation and with no losses

The dynamic permeability tensor referred to the BVMSWs geometry sketched in **Figure 1** is derived from the linearization of the Landau-Lifshitz equation of motion in the magnetostatic limit and in the absence of losses and can be expressed in the form of magneto-gyrotropic media as [8]

$$\mu_{ij} = \begin{pmatrix} \mu_R & 0 & i\mu_I \\ 0 & 1 & 0 \\ -i\mu_I & 0 & \mu_R \end{pmatrix}, \tag{4}$$

where the effective dynamic dependence is separated from the static one ($\mu_{yy} = 1$). The tensor is of rank two and is hermitian. The diagonal components μ_{xx} and μ_{zz} are real with $\mu_{xx} = \mu_{zz} = \mu_R$, where μ_R is the real part of the effective dynamic permeability. We do not deal with the imaginary part that has less physical meaning. Instead, we discuss the trend of μ_R that takes the form [5]:

$$\mu_R(\omega) = \frac{\Omega_{Heff}(1+\Omega_{Heff}) - \Omega^2}{\Omega_{Heff}^2 - \Omega^2}. \quad (5)$$

We restrict ourselves to the underlying physics arising from μ_R for the range of Ω, where it is negative corresponding to the band of BVMSWs. μ_R has a singularity at the Larmor resonance frequency $\Omega = \Omega_{Heff}$ where it diverges negatively, increases for $\Omega_{Heff} < \Omega < (\Omega_{Heff}(1 + \Omega_{Heff}))^{1/2}$ and vanishes in correspondence of the ferromagnetic resonance frequency, namely for $\Omega = (\Omega_{Heff}(1 + \Omega_{Heff}))^{1/2}$. In **Figure 3**, the dependence of μ_R on the angular frequency in the interval $\Omega_{Heff} < \Omega < (\Omega_{Heff}(1 + \Omega_{Heff}))^{1/2}$ is displayed for $\Omega_{Heff} = 0.05$ and $\Omega_{Heff} = 1$ corresponding to frequencies of a few gigahertz for typical magnetic material parameters: $4\pi M = 10^4$ G and $\gamma = 1.76 \times 10^7$ rad/(G s).

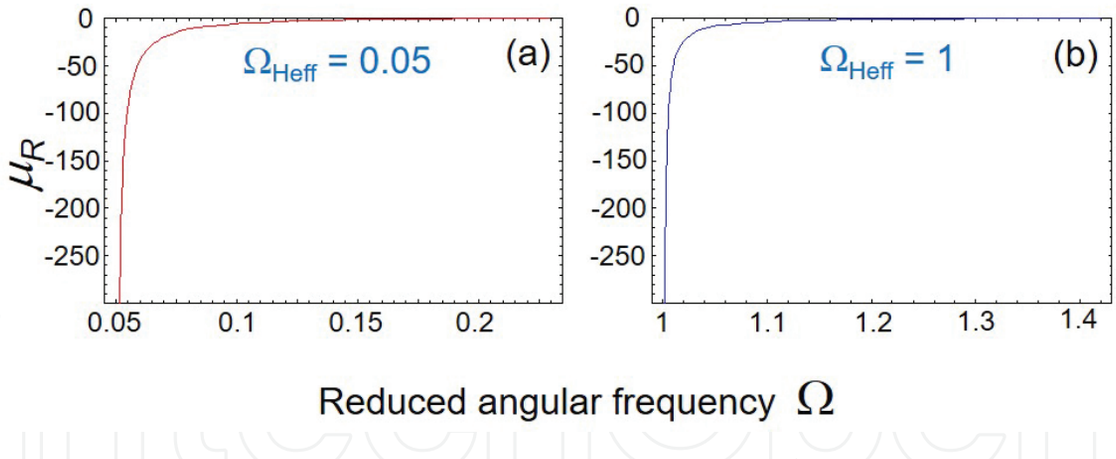

Figure 3. Effective dynamic permeability μ_R for two different values of the effective field. (a) μ_R for $\Omega_{Heff} = 0.05$. (b) μ_R for $\Omega_{Heff} = 1$.

Looking at the two curves, it can be noted that μ_R can be tuned by the external magnetic field intensity.

In conclusion, the study of the peculiar dynamical properties characterizing BVMSWs propagating in ferromagnetic films allows using them as media for coupling electromagnetic radiation in the microwave range with spin excitations. From this point of view, ferromagnetic films can be considered as magnetic metamaterials having properties analogous to those of plasmonic metamaterials where photons are coupled to plasmons.

http://dx.doi.org/10.5772/64070

3. Metamaterial properties of 2D magnonic crystals

This section reports on some recently found metamaterial properties of 2D magnonic crystals (MCs). MCs are prototypes of artificially periodic magnetic systems where the effect of the artificial periodicity is to modify the energy spectrum of collective excitations. MCs can be arranged in one-dimensional (1D), two-dimensional (2D), and three-dimensional (3D) arrays of magnetic nanostructures. In the following sections, the effective properties of 2D antidot lattices (ADLs) recently found by means of micromagnetic simulations and simple analytical calculations are first reviewed and their behavior as metamaterials is highlighted. Finally, bicomponent systems are presented and their interesting recently found effective and metamaterial properties are discussed.

3.1. Magnonic crystals: an introduction

Magnonic crystals are artificially periodic magnetic systems where the artificial periodicity modifies the energy spectrum of collective excitations. Frequency dispersion as a function of the Bloch wave vector strictly depends on the periodicity constant and on the interplay between the dipolar and exchange energy stored in collective modes. At the border of Brillouin zones (BZs), frequency gaps can open such that the propagation is forbidden for specific frequency ranges. There are different kinds of 1D MCs.

The 1D MCs most recently studied in the literature are

1. chains of interacting nanodots of different shapes (see e.g., [12, 13]),
2. arrays of nanostripes (see e.g., [14]).

Instead, the most relevant examples of 2D MCs recently investigated are

3. periodically arranged ferromagnetic nanodots of different shapes interacting along the two in plane directions (see e.g., [15]),
4. antidot lattices (ADLs) where nanoholes of different shapes are periodically embedded into a ferromagnetic matrix (see e.g., [13, 16, 17]),
5. binary systems either composed by nanodots of various shapes and different ferromagnetic materials [21] or formed by nanodots etched into a ferromagnetic matrix of a different material [19, 20].

Finally, note that also 3D MCs consisting of periodic arrangements of ferromagnetic elements of different nature along the three spatial directions have been recently studied (see e.g., [22] where a theoretical analysis on their dynamical properties based on the plane wave method has been performed).

The above-described periodic systems have been also extensively studied experimentally, for instance, by means of Brillouin light-scattering technique and vector network analyzer ferromagnetic resonance technique [11].

In the following section, we focus our attention on recent effective and metamaterial properties found via micromagnetic simulations and supported by analytical calculations. This was done

for ADLs and 2D periodic binary systems. In particular, the static properties have been studied by using Object Oriented MicroMagnetic Framework (OOMMF) code with periodic boundary conditions [23] able to determine the ground-state magnetization for any geometry. Instead, the DMM with implemented 2D periodic boundary conditions [1] has been employed to investigate the dynamical properties with special emphasis on the dynamics of collective modes characterizing these periodic magnetic systems. The DMM is a finite-difference micromagnetic method representing an eigenvalue/eigenvector problem solved in the conservative regime and therefore, for the purposes of the investigation, it aimed to focus on effective and metamaterial properties by neglecting dissipative effects. The frequencies and the profiles of magnonic modes are associated to the eigenvalues and eigenvectors, respectively, of a dynamical matrix obtained in the linear approximation and containing the second-order derivatives of the total energy density calculated at equilibrium. For technical details on the micromagnetic formalism [13]. In these numerical simulations, the equilibrium corresponds to the ground-state magnetization determined via the OOMMF code.

3.2. 2D antidot lattices with in-plane magnetization

In this section, we present some recent theoretical results obtained for the effective properties characterizing 2D ADLs based on the effective medium approximation [17]. Specifically, we deal with a square array of circular holes having nanometric size embedded into a ferromagnetic Permalloy (Py, $Ni_{80}Fe_{20}$) film. The lattice constant is a = 800 nm with holes having diameter d = 120 nm. The Py film thickness is L = 22 nm [16]. Both static and dynamical properties were investigated. To study the system in the effective medium approximation and to extract the effective field, micromagnetic simulations were performed by using OOMMF code for a system composed by 5 × 5 supercells. It has been found that the results of these calculations were exactly reproduced by using the OOMMF code with 2D periodic boundary conditions that were available after these numerical calculations were performed for the first time [23]. The system was subdivided into 5 nm × 5 nm × 22 nm prismatic cells. In the calculation, the typical Py magnetic parameters were used: $4\pi M_s$ = 9.4 kG, $\gamma/2\pi$ = 2.95 GHz/kOe and A = 1.3 × 10^{-6} erg/cm with M_s the saturation magnetization, γ the gyromagnetic ratio, and A the exchange stiffness constant.

For the study of the effective properties the magnetostatic surface wave (MSSW) scattering geometry illustrated in **Figure 4** was considered in the calculations. In this geometry, **H** was applied along the y direction with **H** ⊥ **K** where **K** is the Bloch wave vector of collective modes along the x direction. A magnetic field having intensity H = 200 Oe sufficient to saturate the system (static magnetization **M** parallel to **H** apart from the regions close to the holes) was applied. We denote with region 1 (2), the one in correspondence of (between) vertical rows of holes (see **Figure 4(a)**). The corresponding first Brillouin zone (1 BZ) with the high-symmetry direction ΓX and the high-symmetry points are shown in **Figure 4(b)**.

http://dx.doi.org/10.5772/64070

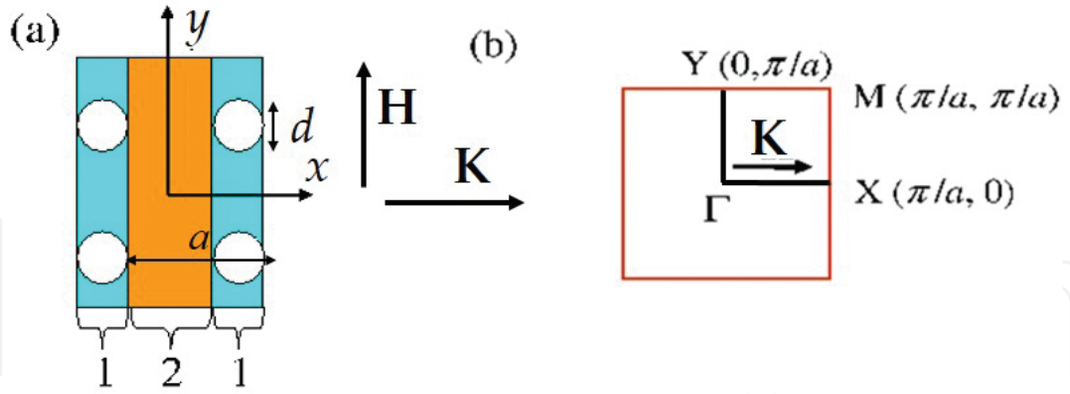

Figure 4. (a) A sketch of the sample regions. Region 1 (blue) corresponds to the vertical rows of ADs. Region 2 (brown) is comprised between the vertical rows of ADs. An in-plane reference frame is also shown together with the directions of **H** and of **K**. (b) 1 BZ with the high-symmetry points and the high-symmetry direction ΓX.

The system can be treated as if it were a continuous magnetic film and effective parameters can be introduced incorporating the effective properties in an effective field arising from the demagnetizing effects associated with holes. For this metamaterial, the dispersion can be written in the approximated form in dimensionless units as

$$\Omega_{MM}^2 = \left(\Omega_{Heff} + \Omega_{Hexch} + f\right)\left(\Omega_{Heff} + \Omega_{Hexch} + 1 - f\right), \tag{6}$$

where $\Omega_{MM} = \omega_{MM}/\omega_M$ with ω_{MM} the angular frequency of the metamaterial (MM) wave, $\omega_M = 4\pi\gamma M_s$ and $\Omega_{Heff} = H_{eff}/4\pi M_s$.

Here, $H_{eff} = H + \langle H_{dem}\rangle$ is the intensity of the effective field given by the sum of the external magnetic field and of the mean demagnetizing (internal) field calculated as an average of its y component over the 128 prismatic cells along the channels comprised between the rows of holes. According to the numerical calculations with OOMMF, it has been found $\langle H_{dem}\rangle \cong -60$ Oe, so that $H_{eff} \cong 140$ Oe. Instead, $\Omega_{Hexch} = H_{exch}/4\pi M_s$ with $H_{exch} = Dk^2$ ($D = 2A/M_s$ is the exchange constant) is the dynamic non-uniform exchange field magnitude and $f = 1\text{-}(1\text{-}\exp(\text{-}KL))/KL$ with the Bloch wave vector $\mathbf{K} = (K, 0)$ aligned along the x direction.

A comparison of the dispersion of the extended modes, the so-called Damon-Eshbach-like (DE_{nBZ}) extended collective modes with $n = 1, 2, \ldots$ (see Section 3.2.1 for a description), calculated by using the DMM, to the one of the metamaterial mode propagating in the channel according to Eq. (6) was made. The DMM micromagnetic calculations were performed in the linear approximation, viz. under the assumption that $\mathbf{M} = \mathbf{M}_0 + \delta\mathbf{m}$, where $\mathbf{M}$ is the total magnetization, $\mathbf{M}_0$ is its static part and the complex dynamic magnetization $\delta\mathbf{m} = (\delta m_x, \delta m_z)$ expresses the small deviations from the ground state. A comparison with the frequencies of the Damon-Eshbach surface mode of the corresponding continuous film calculated in the dipole-exchange regime [3] has also been performed. The results of these calculations are shown in **Figure 5**, and the calculated frequencies are in the microwave range.

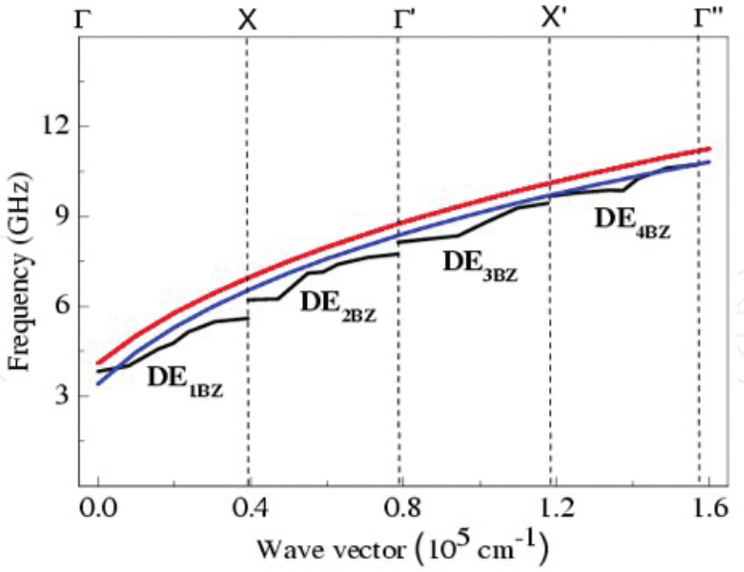

Figure 5. Calculated DMM dispersion of the DE_{nBZ} of the AD lattice (black lines) [16] compared to the calculated Damon-Eshbach dispersion of the unpatterned film (red line) [3] and to the calculated DE dispersion of the MM (blue line) by means of Eq. (6). The edges of BZs are indicated by dashed lines.

At small Bloch wave vectors, the ADL collective mode dynamics (black lines) significantly deviates from the dispersion of the Damon-Eshbach surface mode of the continuous film (red line), while at large Bloch wave vectors, the ADL frequency is closer to that of the Damon-Eshbach mode. Due to demagnetizing effects, the frequencies of the MM mode (blue line) are downshifted with respect to those of the Damon-Eshbach surface mode of the continuous film. The opening of frequency band gaps can be seen at the border of *n*BZs with $n = 1, 2, 3, \ldots$ that can be regarded as another metamaterial property resulting from the artificial periodicity with the band gap amplitude decreasing with increasing n. The band gap opening is mainly due to the inhomogeneity of the internal field in correspondence of the holes, where there is a Bragg diffraction of the Bloch wave for the different families of collective modes including the collective localized modes (not shown) [13, 16].

From an application point of view, because of the explicit dependence on the effective field, the collective mode dispersion calculated according to Eq. (6) could be useful for measuring the internal field experienced by magnonic modes in order to control spin wave propagation in arrays of ADs.

3.2.1. Effective quantities

We now introduce some effective quantities characterizing collective modes. For the sake of simplicity, we restrict ourselves to the analysis of the stationary regime (edges of BZs), but effective quantities can be defined also in the propagative regime (far from BZs edges).

By inspecting spatial profiles, a characteristic wavelength directly related to the scattering with holes can be defined for every collective mode. For hole diameters and for nanometric periodicities, the characteristic wavelength is much larger than hole size. Hence, the charac-

http://dx.doi.org/10.5772/64070

teristic wavelength can be identified as an effective wavelength λ_{eff} defined as the distance between either two maxima or two minima corresponding to the effective periodicity of the wave. In this respect, it is at all effects the wavelength of the wave. Unlike the Bloch wavelength that can assume fractional values of the periodicity, at the edges of the nBZs with $n = 1, 2, \ldots$ the effective wavelength is always commensurable with the array periodicity (it is either equal to a or $2a$). In particular, λ_{eff} characterizes each mode of the spectrum and it is not necessarily equal to the Bloch wavelength $\lambda_B = 2\pi/K$, which decreases with increasing K and becomes comparable to d at high-order nBZs. In the special case studied, d/λ_{eff} is less equal than 0.15 for the whole range of Bloch wave vectors investigated. Correspondingly, collective modes have also a small effective wave vector $\mathbf{k}$ of modulus $k = 2\pi/\lambda_{eff}$ that is not necessarily equal to the Bloch wave vector of modulus $k = 2\pi/\lambda_B$. By means of this small effective wave vector, the influence of holes acting as scattering centers on collective spin modes is expressed in an even more direct way with respect to that of the effective wavelength.

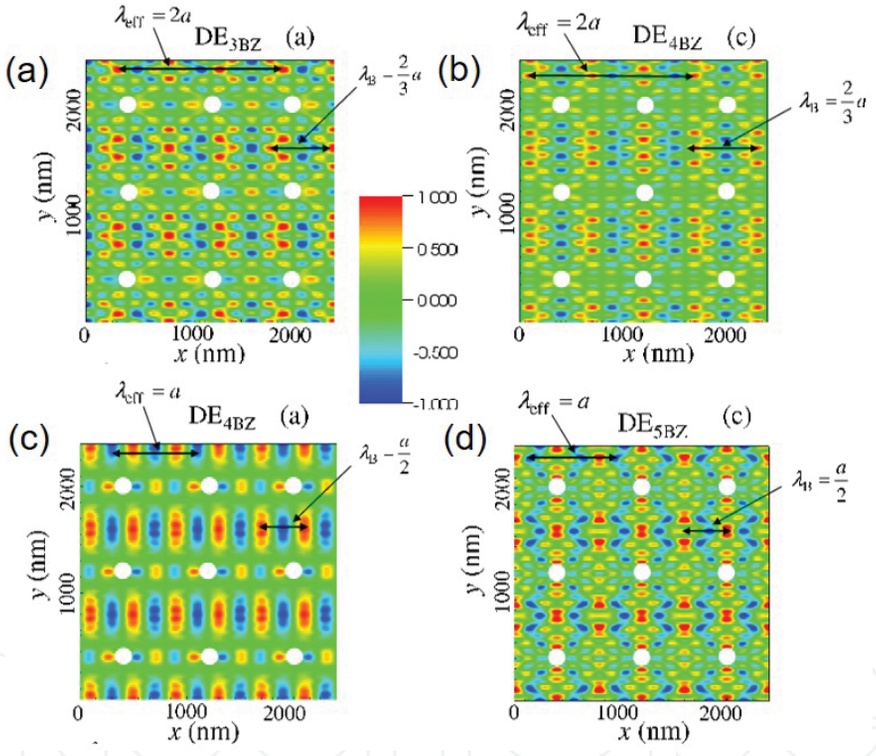

Figure 6. Spatial profiles (Re[δm_z]) of collective modes. (a) DE_{3BZ} mode at the edge of the 3 BZ. (b) DE_{4BZ} mode at the edge of the 3 BZ. (c) DE_{4BZ} mode at the edge of the 4 BZ. (d) DE_{5BZ} mode at the edge of the 4 BZ. For each collective mode the effective wavelength λ_{eff} and the Bloch wavelength λ_B are indicated.

Two examples underlining the difference between the meaning of the effective wavelength and of the Bloch wavelength and the corresponding wave vectors for the array of ADs studied are shown in **Figure 6**, where two couples of the so-called extended modes exhibiting large amplitude in the horizontal channels comprised between hole rows and non-negligible amplitude in the rows are depicted at nBZs edges with $n = 3, 4$. In particular, the calculated spatial profiles of the couple of extended modes DE_{3BZ} and DE_{4BZ} at the X' point (border of 3

BZ, n = 3) and of the couple of extended modes DE_{4BZ} and DE_{5BZ} at the Γ'' point (border of 4 BZ) are shown. The numerical frequencies are ν = 9.44 GHz for the DE_{3BZ} and ν = 9.67 GHz for the DE_{4BZ} with a band gap of amplitude of 0.23 GHz. Looking at the spatial profiles of DE_{3BZ} and DE_{4BZ}, their effective wavelength is three times the Bloch wavelength λ_B both in the horizontal rows and in the horizontal channels, namely λ_{eff} =2a. Instead, from the inspection of the spatial profiles, the effective wavelength of DE_{4BZ} and DE_{5BZ} modes is λ_{eff} =a, both in the horizontal rows and horizontal channels, and is twice the Bloch wavelength. The numerical frequencies are ν = 10.70 GHz for DE_{4BZ} and ν = 10.83 GHz for DE_{5BZ} with a band gap of amplitude of 0.13 GHz. For each couple of modes, the amplitudes are phase shifted of π/2. Similar conclusions are drawn by studying the spatial profiles of collective localized modes whose spatial profiles have larger amplitudes in the horizontal rows of holes [13, 16].

For a discussion of other effective properties characterizing ADLs [17]. The same features remain valid for other types of ADLs in the nanometric and submicrometric ranges having different hole shape, periodicity, type of unit cell, and ferromagnetic materials. They remain valid also for other scattering geometries depending on the relative orientation of **K** with respect to **H** including the BVMSW scattering geometry (**K** || **H**) and for other high-symmetry directions in the reciprocal space [17, 24].

Moreover, similar numerical results have been obtained for perpendicularly magnetized thin CoFeB ADLs with strong uniaxial perpendicular anisotropy [18]. This means that the effective description of ADLs dynamics does not depend on the ground-state magnetization. For a quantitative description of the relations between the effective quantities and the corresponding Bloch quantities together with other general rules valid for the types of 2D periodic systems reviewed in this chapter (see Section 3.4).

3.3. Binary and periodic ferromagnetic systems: Py/Co and Co/Py

In this section, we describe the recent results found according to micromagnetic simulations carried out by means of DMM on the effective properties of binary and periodic ferromagnetic systems [19, 20] that can be regarded as another class of magnetic metamaterials. In particular, it is shown that also in these systems, the dynamics of the most representative collective modes in the effective medium approximation can be described in terms of an MM propagating wave. This is done in analogy with what occurs in ADLs with, in addition, the definition of other effective quantities directly related to the presence of two ferromagnetic materials. We report here the geometry of a Py/Co binary and periodic system with periodicity a = 600 nm, where a periodic arrangement of Co circular dots are embedded into a Py matrix. The Co circular dots have diameters d= 310 nm and are totally etched into the Py film while the thickness of the continuous film is L_{Py} = 16 nm for every system. The ground-state magnetization has been determined by using the OOMMF code with periodic boundary conditions [23]. In the simulations, prismatic cells of 7.5 nm × 7.5 nm × 8 nm size have been used subdividing the thickness into a stack of two layers. The magnetic parameters used in the simulations range within the typical values of the literature. For Py, $\gamma_{Py}/2\pi$ = 2.96 GHz/kOe, $M_{s,Py}$ = 740 emu/cm^3, and A_{exch}^{Py} = 1.3 × 10^{-6} erg/cm, while for Co, $\gamma_{Co}/2\pi$ = 3.02 GHz/kOe, $M_{s,Co}$ = 1000 emu/cm^3, and

http://dx.doi.org/10.5772/64070

$A_{exch}^{Co} = 1.5 \times 10^{-6}$ erg/cm (this value is typical of polycrystalline Co). Micromagnetic simulations have been carried out for an external in-plane magnetic field **H** applied along the y direction having intensity $H = 500$ Oe.

In order to find the frequency dispersion of the metamaterial wave, it is useful to define an effective magnetization by means of the filling ratio $\eta = \pi R^2/a^2$, where R is the dot radius, namely:

$$M_{eff} = M_{s,Py}(1-\eta) + M_{s,Co}\eta. \tag{7}$$

In addition, it can be defined also an effective magnetic field that plays the role of an internal field experienced by the MM wave and depends on both materials:

$$H_{eff} = H + < H_{dem}^{y} >, \tag{8}$$

where $< H_{dem}^{y} >$ denotes the average of the y component of the static demagnetizing field over the 80 prismatic cells of the unit cell along both x and y directions due to its uniformity along the z direction. Because of its small contribution, the static exchange field can be safely neglected. The effective gyromagnetic ratio and the effective stiffness constant are $\gamma_{eff} \approx \gamma_{Py}$ and $A_{eff} \approx A_{exch}^{Py}$, respectively.

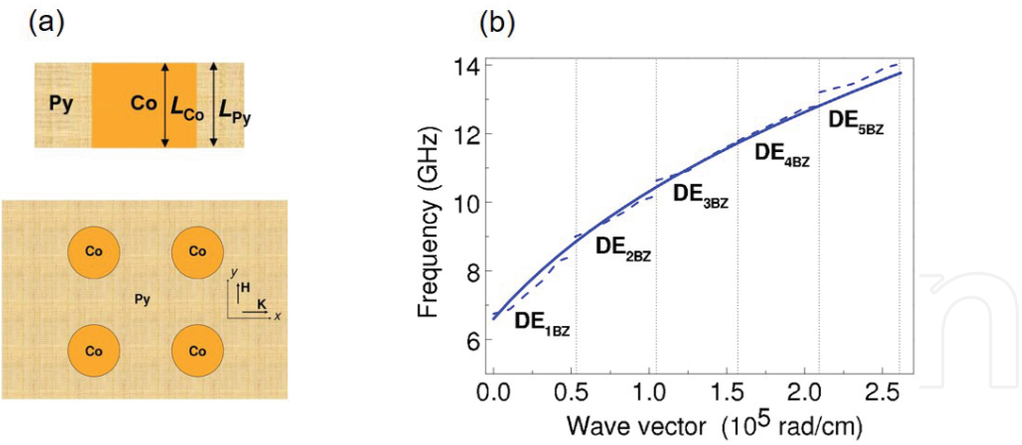

Figure 7. (a) Pictorial sketch and top view of the Py/Co system and (b) calculated DMM frequency dispersion of the DE_{nBZ} modes (dashed blue lines) for Py/Co system compared to the Damon-Eshbach dispersion of the MM mode (solid blue line) calculated according to Eq. (6) and accounting for Eqs. (7) and (8).

The frequency dispersion of the MM wave can be calculated according to Eq. (6) by taking into account Eqs. (7) and (8), $L = L_{Py}$, L_{Co}, $\gamma \approx \gamma_{Py}$, and $A \approx A_{exch}^{Py}$ and corresponds to the effective medium description of the DE_{nBZ} collective modes having an appreciable amplitude in the whole unit cell. **Figure 7(a)** shows a sketch of the Py/Co system studied. In **Figure 7(b)**, the

MM wave dispersion is compared to the DE_{nBZ} dispersion obtained according to DMM with implemented 2D boundary conditions and extended to systems composed by several materials [20]. The numerical values obtained from micromagnetic simulations are H_{eff} = 476 Oe being $<H_{dem}^{y}>$ = -24 Oe, and M_{eff}= 794 emu/cm^3. The calculated frequency intersects, at the nBZ borders, the middle frequency of the corresponding band gaps determined by means of DMM with the only exception of the 5 BZ. For the micromagnetic simulations on the other families of collective modes and on the other types of binary periodic Py/Co and Co/Py systems with different filling fractions [19, 20].

3.3.1. Effective "surface magnetic charges"

In this section, we recall the definition of effective "surface magnetic charges" recently introduced [20] that can be applied to binary and periodic ferromagnetic systems. As an example, we discuss their distribution for the Py/Co system of the previous paragraph and of the Co/Py system obtained by interchanging the two ferromagnetic materials. By considering the Py/Co system at the border of Co cylindrical dots, an effective "surface magnetic charge" density can be defined as the linear superposition of the "surface magnetic charge" densities of the two ferromagnetic materials, viz. $\sigma_{eff}=\mathbf{M}_{Py}\cdot\hat{n}+\mathbf{M}_{Co}\cdot\hat{n}'$. Here, $\hat{n}$ is the unit vector associated to $\mathbf{M}_{Py}$ external to Py film, but internal to Co cylindrical dot, while $\hat{n}'$ is the corresponding unit vector associated to $\mathbf{M}_{Co}$ external to Co cylindrical dot, but internal to Py film.

σ_{eff} can be expressed in the simple form:

$$\sigma_{eff} = \Delta\mathbf{M}_{Co\text{-}Py}\cdot\hat{n}', \tag{9}$$

via $\hat{n}=-\hat{n}'$ with the vector $\Delta\mathbf{M}_{Co\text{-}Py}=\mathbf{M}_{Co}-\mathbf{M}_{Py}$. The effective "surface magnetic charge" density is thus proportional to the difference between the magnetizations of the two ferromagnetic materials.

In **Figure 8(a)**, the distribution of the "surface magnetic charges" is depicted together with the direction of **H** for the Py/Co system. The magnetic field applied along the y axis orients along the same direction both the static magnetization in the Py film and the one inside the Co cylindrical dots, $\mathbf{M}_{Py}$ and $\mathbf{M}_{Co}$, respectively. This leads to the formation of "surface magnetic charges" of opposite sign, but of different magnitude at the interface between Py and Co. The net effect is the formation of what we call effective "surface magnetic charges" that take the signs of the "surface magnetic charges" due to $\mathbf{M}_{Co}$, because of the larger value of $M_{s,Co}$ with respect to $M_{s,Py}$. This effect is pictorially shown in **Figure 8**. Note that the ground-state magnetization exhibits a slight deviation from the collinear state close to the dot surface at the border between the two materials as found according to micromagnetic simulations performed with OOMMF and this effect is not shown in **Figure 8**.

http://dx.doi.org/10.5772/64070

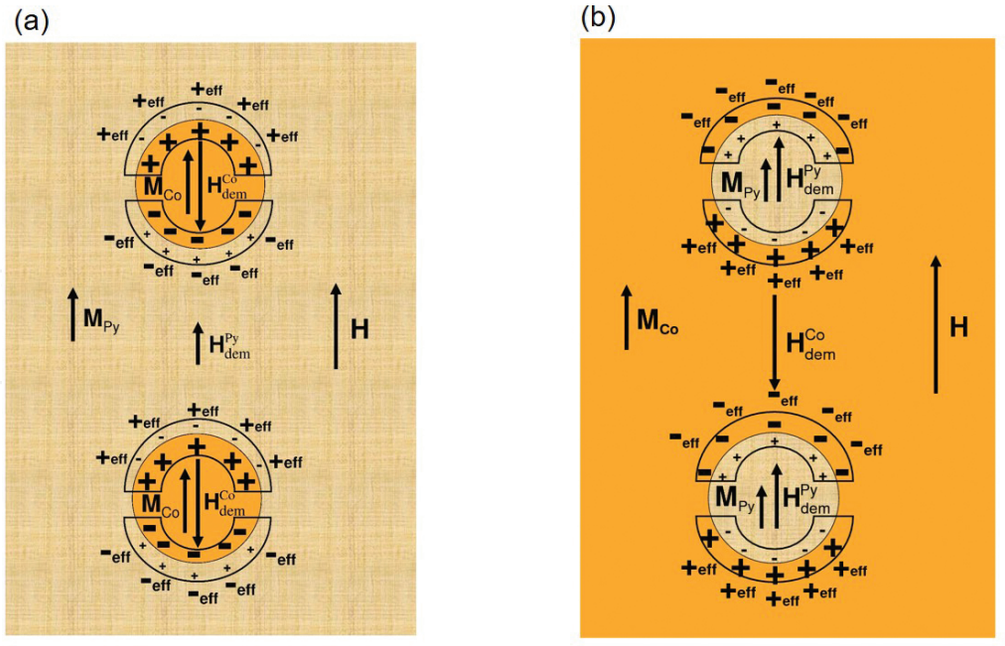

Figure 8. (a) Top view of the distribution of "surface magnetic charges" for the Py/Co system. The positive and negative effective "surface magnetic charges" are shown. The subscript "eff" stands for "effective." The directions of $\mathbf{M}_{Py}$, $\mathbf{M}_{Co}$, and $\mathbf{H}$ together with those of the Co and Py static demagnetizing fields $\mathbf{H}^{Co}_{dem}$ and $\mathbf{H}^{Py}_{dem}$, respectively, are also displayed. (b) As in panel (a) but for the Co/Py system. The meaning of the symbols is the same.

By interchanging the two ferromagnetic materials (Co/Py system), the corresponding distribution of effective "surface magnetic charges" becomes opposite to that of Py/Co system (see **Figure 8(b)**). Again, the effective "surface magnetic charges" at the interface between Py and Co take the sign of those of Co, because the "surface magnetic charge" density due to Co at the interface is higher with respect to that of Py. As a result, there is a reversal of the orientations of $\mathbf{H}^{Py}_{dem}$ and $\mathbf{H}^{Co}_{dem}$ static demagnetizing fields with respect to the corresponding $\mathbf{H}^{Co}_{dem}$ and $\mathbf{H}^{Py}_{dem}$ ones of Py/Co system, respectively. As a consequence of the formation of effective "surface magnetic charges," in both systems shown in **Figure 8**, the Py static demagnetizing field is parallel to $\mathbf{M}_{Py}$, while the Co static demagnetizing field $\mathbf{H}^{Co}_{dem}$ is antiparallel to $\mathbf{M}_{Co}$. Note that, for both Py/Co and Co/Py systems, $\mathbf{H}^{Py}_{dem}$ ($\mathbf{H}^{Co}_{dem}$) is not only due to Py (Co) but also due to their combined effect mainly related to the nonlocal nature of demagnetizing fields. For a discussion about the effective "surface magnetic charges" of other types of Py/Co or Co/Py systems characterized by other filling fractions [20].

The definition of effective "surface magnetic charges" allows to introduce an effective magnetic potential that is expressed in terms of both the "volume magnetic charges" and the effective "surface magnetic charges." By taking into account the non-collinearity of the ground-state magnetization that gives rise to volume contributions and its three-dimensional spatial dependence, the effective magnetic potential gets its contributions from two volume integrals, one for each ferromagnetic material, and from one surface integral. For Py/Co system, it reads:

$$\Phi_{\mathrm{M}}^{\mathrm{Py/Co}}\left(\mathbf{r}\right) = -\int\limits_{V_{\mathrm{cell}}-V_{\mathrm{dot}}} \frac{\nabla\cdot\mathbf{M}_{\mathrm{Py}}}{\left|\mathbf{r}-\mathbf{r}''\right|}d\mathbf{r}'' - \int\limits_{V_{\mathrm{dot}}} \frac{\nabla\cdot\mathbf{M}_{\mathrm{Co}}}{\left|\mathbf{r}-\mathbf{r}''\right|}d\mathbf{r}'' + \int_{S}\frac{\sigma_{\mathrm{eff}}}{\left|\mathbf{r}-\mathbf{r}''\right|}d\mathbf{S}'', \tag{10}$$

where **r**= (*x*, *y*, *z*) and *S* is the lateral surface in common between the two ferromagnetic materials. For the sake of simplicity, the dependence on the spatial coordinate in the integrand functions on the second member appearing at the numerators is omitted. It is interesting to note a main difference between the volume contributions and the surface contributions. While for the volume contributions it is possible to separate the first two terms on the second member coming from the two ferromagnetic materials, this is not anymore true for the last term related to the surface contribution. Indeed, the last term is proportional to the effective "surface magnetic charge" density depending on the contrast between the magnetizations of the two ferromagnetic materials expressed by Eq. (9). By interchanging the two ferromagnetic materials, the effective magnetic potential of Eq. (10) is not invariant, that is $\Phi_{\mathrm{M}}^{\mathrm{Co/Py}} \neq \Phi_{\mathrm{M}}^{\mathrm{Py/Co}}$. The lack of invariance is due to the two volume contributions appearing in the first and second integral on the second member that change their values upon interchanging Py with Co. Instead, the effective potential is invariant if it is supposed a quasi-collinear distribution of the magnetization leading to the neglect of the volume contributions. In this case, it is:

$$\Phi_{\mathrm{M}}^{\mathrm{Py/Co}}\left(\mathbf{r}\right) = \Phi_{\mathrm{M}}^{\mathrm{Co/Py}}\left(\mathbf{r}\right) = \int_{S}\frac{\sigma_{\mathrm{eff}}}{\left|\mathbf{r}-\mathbf{r}''\right|}d\mathbf{S}''. \tag{11}$$

Indeed, the magnetic potential depends only on the difference in modulus of the saturation magnetization of the two materials according to the definition of σ_{eff} (Eq. (9)).

3.4. General quantitative relations for effective quantities in ferromagnetic ADLs and binary and periodic magnonic crystals

For the two types of 2D magnonic crystals studied previously and represented by square lattices, it is possible to express some general quantitative relations involving the effective quantities characterizing the dynamics of collective modes for the scattering geometries investigated and for the two different ground-state magnetizations (either in-plane or perpendicular to the plane). First, some general rules between the effective quantities and the corresponding Bloch quantities have been found. These rules have been rigorously proved looking at the spatial profiles of each family of collective modes in the stationary regime (at *n*BZs boundaries). They are summarized as follows:

a. The effective wavelength is a function of the Bloch wavelength [19], viz.

http://dx.doi.org/10.5772/64070

$$\lambda_{\text{eff}}^{n\text{BZ}} = \begin{cases} n\lambda_{\text{B}}^{n\text{BZ}} & \text{if } n \text{ is odd} \\ \frac{n}{2}\lambda_{\text{B}}^{n\text{BZ}} & \text{if } n \text{ is even} \end{cases}. \tag{12}$$

At the *n*BZs edges, the effective wavelength is commensurable with the periodicity and assumes either the value $2a$ or a depending on n with $n = 1, 2, \ldots$

b. The small effective wave vector can be written in terms of the Bloch wave vector for odd and even BZs edges, respectively [17]:

$$\mathbf{k}^{(2l+1)\text{BZ}} = \mathbf{K}^{(2l+1)\text{BZ}} - \mathbf{G}; \;\; \mathbf{k}^{(2l+2)\text{BZ}} = \mathbf{K}^{(2l+2)\text{BZ}} - \mathbf{G} \tag{13}$$

where $\mathbf{G} = (l\, b^x, 0)$, $l = 0, 1, 2, \ldots$ and $b^x = 2\pi/a$. The small effective wave vector $\mathbf{k}$ can be interpreted as a Bloch wave vector shifted by a reciprocal lattice vector $\mathbf{G}$, but not necessarily shifted into the 1 BZ and at the *n*BZs, edges assumes either the value $\mathbf{k} = (\pi/a, 0)$ for n odd with $n = 1, 3, \ldots$ or the value $\mathbf{k} = (2\pi/a, 0)$ for n even with $n = 2, 4, \ldots$ It has been found that as the hole size tends to zero (about 10 nm), the effective wavelength becomes equal to the Bloch wavelength (and the same for the corresponding effective wave vectors) and, in this limit, the description of the spin dynamics in terms of effective properties is not anymore valid [17]. This is also true when the size of the inclusion (dot) in a binary magnonic crystal becomes very small, but it is still not zero. When the size of the defect vanishes, the role of the Bloch quantities is replaced by those of the wavelength of the surface Damon-Eshbach wave and of the corresponding propagating wave vector in a continuous ferromagnetic film. In principle, the above relations between the effective quantities and the Bloch quantities expressed by Eq.(12) and Eq.(13) can be extended also to the case when **H** and **K** are, for example, along the diagonal of the square cell in the MSSW scattering geometry corresponding to the ΓM direction in the reciprocal space. However, in this latter case, it has been proved, according to symmetry arguments for the case of square ADLs, that the effective wavelength of the collective modes is twice the effective periodicity and is not anymore commensurable with it [24].

As a consequence of the previous described effective rules, some further general relations can be extracted in the stationary regime [17]. In particular,

i. An effective rule on the dynamic magnetization.

ii. An inequality between the effective wavelength and the Bloch wavelength and as a consequence between the small effective wave vector and the Bloch wave vector.

iii. A quantitative representation of the dynamic magnetization components of collective modes in terms of the effective wavelength.

Concerning (i), it is possible to prove an effective rule on the dynamic magnetization, analogous to the well-known Bloch rule where the small effective wave vector appears in place of the Bloch wave vector, viz.

$$\delta\mathbf{m}_{\mathbf{k}}\left(\mathbf{r}+\mathbf{R}\right)=\delta\mathbf{m}_{\mathbf{k}}\left(\mathbf{r}\right)\exp^{i\mathbf{k}\cdot\mathbf{R}}, \tag{14}$$

where **R** is the translational vector of the periodic system and, for the sake of simplicity, the superscript in the small effective wave vector has been omitted. Indeed, according to Eq. (13), it is always $\exp^{i\mathbf{K}\cdot\mathbf{R}}=\exp^{i\mathbf{k}\cdot\mathbf{R}}=\mp 1$, where −1 refers to odd edges of *n*BZs (*n* = 1, 3, …) and +1 to even edges of BZs (*n*= 2, 4, …). Therefore, at the edges of *n*BZs, the phase factor of the Bloch function remains unchanged if the Bloch wave vector is replaced by the corresponding small effective wave vector. Straightforwardly, from the effective rule expressed by Eq. (14), it can be shown that the well-known Bloch rule is fulfilled. Indeed, by using Eq. (13) and omitting the superscripts, Eq. (14) takes the form:

$$\delta\mathbf{m}_{\mathbf{K}}\left(\mathbf{r}+\mathbf{R}\right)=\delta\mathbf{m}_{\mathbf{K}}\left(\mathbf{r}\right)\exp^{i(\mathbf{K}-\mathbf{G})\cdot\mathbf{R}}=\delta\mathbf{m}_{\mathbf{K}}\left(\mathbf{r}\right)\exp^{i\mathbf{K}\cdot\mathbf{R}}, \tag{15}$$

since $\exp^{-i\mathbf{G}\cdot\mathbf{R}}=1$ for each reciprocal lattice vector **G**. Notice that the vector **G** does not necessarily coincide with the well-known **G** used to pass from the extended to the reduced zone scheme.

We now discuss (ii). A general relation can be found from the analysis of the effective wavelength and of the corresponding small effective wave vector. Independently of the collective mode considered, the effective wavelength is always larger than or equal to the Bloch wavelength, viz.

$$\lambda_{\mathrm{eff}}\geq\lambda_{\mathrm{B}}. \tag{16}$$

Hence, a scattering selection rule can be established. Due to the presence of a periodic arrangement of finite size defects (either in the form of holes or in the form of dots having size in the nanometric range and smaller than the lattice constant of the 2D magnonic crystal), it is not allowed for a magnonic wave that scatters on the defect to have an effective wavelength smaller than the Bloch wavelength. Even though not yet investigated in detail, this rule is fulfilled in 2D square arrays of ADLs and in binary and periodic systems independently of the holes shape and of the dots shape and material. It has been proved to be independent also on the studied scattering geometry, viz. MSSW (**K** ⊥ **H**) or MSBVW (**K** ∥ **H**) with **H** oriented either along the rows of holes in ADLs and of dots in binary periodic systems or along the diagonal of the square cell. This can be regarded as a general metamaterial property of 2D periodic magnetic systems where finite size defects act as scattering centers. From the inequality of Eq.

http://dx.doi.org/10.5772/64070

(16), the following general inequality between the magnitude of the small effective wave vector and that of the Bloch wave vector **K** can be written, viz.

$$k \leq K. \tag{17}$$

For both relations, the equality holds at the edge of 1 BZ and 2 BZ, while from the edge of 3 BZ ahead, the strict inequality is fulfilled.

Regarding (iii), strictly related to the effective rule discussed in (i) and to the above relations involving the effective quantities described in (ii), also a quantitative representation of the dynamic magnetization of collective modes in terms of the effective wavelength can be given. It is possible to give a simple representation of the components of the dynamic magnetization associated to collective modes for both types of 2D magnonic crystals presented and for the MSSW scattering geometries described at the edges of BZs (including the one along the ΓM high-symmetry direction) in terms of the effective quantities. In particular:

$$\delta m_i = A_i \sin\left(\mathbf{k}\cdot\mathbf{r}\right) = A_i \sin\left(\mathbf{k}\cdot\left(\mathbf{r}+\mathbf{r}_{\text{eff}}\right)\right), \tag{18}$$

$$\delta m_i = A_i \cos\left(\mathbf{k}\cdot\mathbf{r}\right) = A_i \cos\left(\mathbf{k}\cdot\left(\mathbf{r}+\mathbf{r}_{\text{eff}}\right)\right), \tag{19}$$

with $i = x, z$. Here, A_i is a complex amplitude (either purely real or purely imaginary) and in the MSSW scattering geometry with the Bloch wave vector **K** along the x direction, it is $\mathbf{r} = (x, 0)$, $\mathbf{k} = (k_x, 0)$, and $\mathbf{r}_{\text{eff}} = (x_{\text{eff}}, 0)$ so that $\lambda_{\text{eff}} = x_{\text{eff}}$. This representation is not only valid for describing collective modes in 2D ADLs whose dynamics is studied in the MSSW scattering geometry [17], but it can be also extended to the MSBVW scattering geometry and to the collective mode dynamics in the binary periodic magnetic systems discussed previously for the same scattering geometries.

4. Applications of 2D magnonic crystals as metamaterials

In this section, we briefly discuss some possible future applications of 2D magnonic crystals based on their metamaterial properties [17]. First, we describe the realization of a magnonic device exploiting the definition of the small effective wave vector that could potentially open the route for experiments on collective modes mapping. Second, we propose a technique based on the Fourier analysis for mapping the spatial profiles of magnonic modes as already done for spin-wave modes in isolated magnetic vortex-state disks [25] and in 2D arrays of saturated magnetic nanoelements [26].

4.1. Magnonic metamaterial device

The fabrication of a magnonic device able to exploit the definition of the small effective wave vector is proposed. As usual, the magnonic device consists of three regions. The first region is an input region, represented by an antenna producing a small magnetic field $\mathbf{h}(\mathbf{r}, t)$ having a spatial dependence proportional to $\exp^{i\boldsymbol{\kappa}\cdot\mathbf{r}}$ with $\boldsymbol{\kappa}$ the wave vector and a time dependence of the form $\exp^{i\omega_R t}$ with a resonance angular frequency ω_R. Instead, the second region is a functional region manipulated by the external magnetic field containing the 2D magnonic crystal under study, while the last region is an output region where the microwave signal is collected. Importantly, the resonance condition on the wave vector can be expressed in terms of the small effective wave vector previously discussed, namely $\boldsymbol{\kappa} = \mathbf{k}$. Hence, it is sufficient to use the only two values $\mathbf{k} = (\pi/a, 0)$ and $\mathbf{k} = (2\pi/a, 0)$ corresponding to wavelengths of $2a$ and a, respectively, to excite all the couples of modes of interest separated by band gaps at the border of the nBZ. Indeed, the number of values of Bloch wave vectors $\mathbf{K} = (n\pi/a, 0)$ with $n = 1, 2, 3, \ldots$ at nBZ edges that should be employed would be greater. Exploiting the resonance condition on the frequency ω_R of the oscillating field, the frequencies of a couple of modes corresponding to a BZ edge and separated by a gap can be obtained and distinguished from the frequencies of another couple of modes belonging to another BZ edge. Therefore, the spatial and temporal resonance mechanism could permit to make a mapping of the frequencies of collective modes of 2D magnonic crystals independently of the geometry studied.

4.2. Imaging of collective modes

We suggest an experiment to confirm the predictions of micromagnetic simulations obtained by means of the DMM about the main features of spatial profiles of collective modes. The proposed experiment is similar to the one carried out, for example, for mapping spin-wave modes in isolated disks in the vortex state [25] or in 2D arrays of magnetic nanoelements in the saturated state [26]. By applying a magnetic field pulse with an in-plane component and by Fourier transforming the time domain signal recorded at each location of the unit cell into the frequency domain, the modal structure of the most representative collective excitations in the 2D magnonic crystals previously described could be measured. From this procedure, a spatial map of Fourier amplitudes and phases of collective modes could be determined and compared to micromagnetic spatial profiles. By means of this experimental analysis, it could be also investigated for 2D periodic magnetic systems the role of point defects in the form of either holes or magnetic dots of different shapes in determining the effective properties of collective modes like, for instance, the effective wavelength and its commensurability with the periodicity of the system. This experimental analysis could highlight further effective properties not yet theoretically investigated.

5. Conclusions

In summary, in this chapter, a systematic overview of the static and dynamical properties of 2D magnetic nanostructures has been made. The overview has included the theoretical analysis

http://dx.doi.org/10.5772/64070

of spin-wave modes having backward character and the investigation of effective properties of collective modes in 2D periodic systems. According to the presented results, a description of the dynamical features of continuous films and 2D magnonic crystals in terms of effective and metamaterial properties has been done. In the case of continuous ferromagnetic films, special emphasis has been given mainly to the metamaterial properties related to BVMSWs having "negative" group velocity in the purely dipolar regime and negative effective dynamic permeability. Instead, for the 2D magnonic crystals investigated, effective quantities and effective rules have been found starting from the inspection of the spatial profiles of collective modes and the role of holes and of ferromagnetic inclusions acting as scattering centers has been highlighted. In this respect, 2D magnetic nanostructures can be regarded as a new class of metamaterials that can be put on a similar footing as, for instance, other classes of widely studied metamaterials such as plasmonic, dielectric, and electromagnetic metamaterials. The found properties could open the route for further experimental investigations in the field of magnonic crystals such as, for instance, the mapping of collective excitations of different kinds and for different geometries and can be exploited for tailoring a magnonic device able to confirm the theoretical predictions on the effective quantities and effective properties characterizing collective spin-wave modes.

Acknowledgements

This work was partially supported by National Group of Mathematical Physics (GNFM-INdAM). The author acknowledges L. Giovannini for making available the DMM micromagnetic code.

Author details

Roberto Zivieri

Address all correspondence to: roberto.zivieri@unife.it

Department of Physics and Earth Sciences, University of Ferrara, Ferrara, Italy

References

[1] Giovannini L, Montoncello F, Nizzoli F: Effect of interdot coupling on spin-wave modes in nanoparticle arrays. Phys. Rev. B. 2007; 75: 024416. DOI: 10.1103/PhysRevB.75.024416

[2] Damon RW, Eshbach JR: Magnetostatic modes of a ferromagnet slab. J. Phys. Chem. Solids. 1961; 19: 308–320. DOI: 10.1016/0022-3697(61)90041-5

[3] Kalinikos BA, Slavin AN: Theory of dipole-exchange spin wave spectrum for ferromagnetic films with mixed exchange boundary conditions. J. Phys. C. 1986; 19: 7013–7033. DOI: 10.1088/0022-3719/19/35/014

[4] Zivieri R. Magnetic matter spin waves with "negative" group velocity. In: Proceedings of the 9th International Congress on Advanced Electromagnetic Materials and Optics (Metamaterials' 2015); 7–10 September 2016; Oxford. 2015. pp. 529–531. DOI: 10.1109/MetaMaterials.2015.7342512 04/04/2016 http://ieeexplore.ieee.org/xpl/articleDetails.jsp?arnumber=7342512

[5] Zivieri R. Dynamic negative permeability in a lossless ferromagnetic medium. In: Proceedings of the 9th International Congress on Advanced Electromagnetic Materials and Optics (Metamaterials' 2015); 7–10 September 2016; Oxford. 2015. pp. 532–534. DOI: 10.1109/MetaMaterials.2015.7342513 04/04/2016 http://ieeexplore.ieee.org/xpl/articleDetails.jsp?arnumber=7342513

[6] Veselago VG: The electrodynamics of substances with simultaneously negative values of ε and μ. Sov. Phys. Usp. 1968; 10: 509–515. DOI: 10.1070/PU1968v010n04ABEH003699

[7] Alù A, Engheta N: Pairing an epsilon-negative slab with a mu-negative slab: resonance, tunneling and transparencies. IEEE Trans. Antennas Propag. 2003; 51: 2558–2571. DOI: 10.1109/TAP.2003.817553

[8] Mikhaylovskiy RV, Hendry E, Kruglyak VV: Negative permeability due to exchange spin-wave resonances in thin magnetic films with surface pinning. Phys. Rev. B 2010; 82: 195446. DOI: 10.1103/PhysRevB.82.195446

[9] Nikitov SA, Tailhades P, Tsai CS: Spin waves in periodic magnetic structures magnonic crystals. J. Magn. Magn. Mater. 2001; 236: 320–330. DOI: 10.1016/S0304-8853(01)00470-X

[10] Elachi C: Magnetic wave propagation in a periodic medium. IEEE Trans. Magn. Magn. 1975; 11: 36–39. DOI: 10.1109/TMAG.1975.1058546

[11] Kruglyak VV, Demokritov SO, Grundler D: Magnonics. J. Phys. D: Appl. Phys. 2010; 43: 264001. DOI: 10.1088/0022-3727/43/26/264001

[12] Zivieri R, Montoncello F, Giovannini L, Nizzoli F, Tacchi S, Madami M, Gubbiotti G, Carlotti G, Adeyeye AO: Collective spin modes in chains of dipolarly interacting rectangular magnetic dots. Phys. Rev. B 2011; 83: 054431. DOI: 10.1103/PhysRevB.83.054431

[13] Zivieri R: Metamaterial properties of one-dimensional and two-dimensional magnonic crystals. Sol. State Phys. 2012; 63: 151–216. DOI: 10.1016/B978-0-12-397028-2.00003-5

[14] Wang ZK, Zhang VL, Lim HS, Ng SC, Kuok MH, Jain S, Adeyeye AO: Observation of frequency band gaps in a one-dimensional nanostructured magnonic crystal. Appl. Phys. Lett. 2009; 94: 083112. DOI: 10.1063/1.3089839

[15] Tacchi S, Montoncello F, Madami M, Gubbiotti G, Carlotti G, Giovannini L, Zivieri R, Nizzoli F, Jain S, Adeyeye AO, Singh N: Band diagram of spin waves in a two-dimensional magnonic crystal. Phys. Rev. Lett. 2011; 107: 127204. DOI: 10.1103/PhysRevLett.107.127204

[16] Zivieri R, Tacchi S, Montoncello F, Giovannini L, Nizzoli F, Madami M, Gubbiotti G, Carlotti G, Neusser S, Duerr G, Grundler D: Bragg diffraction of spin waves from a two-dimensional antidot lattice. Phys. Rev. B 2012; 85: 012403. DOI: 10.1103/PhysRevB.85.012403

[17] Zivieri R, Giovannini L: Effective quantities and effective rules in two-dimensional antidot lattices. Photon. Nanostruct. Fundam. Appl. 2013; 11: 191–202. DOI: 10.1016/j.photonics.2013.07.002

[18] Malagò P, Giovannini L, Zivieri R. Perpendicularly magnetized antidot lattice as a two-dimensional magnonic metamaterial. In: Proceedings of the 9th International Congress on Advanced Electromagnetic Materials and Optics (Metamaterials' 2016); 7–10 September 2016; Oxford. 2015. pp. 532–534. DOI: 10.1109/MetaMaterials.2015.7342513 04/04/2016 http://ieeexplore.ieee.org/xpl/articleDetails.jsp?arnumber=7342514

[19] Malagò P, Giovannini L, Zivieri R. Effective properties of a binary magnonic crystal. In: Proceedings of the 8th International Congress on Advanced Electromagnetic Materials and Optics (Metamaterials' 2014); 25–30 August 2014; Copenhagen. 2014. pp. 316–318. DOI: 10.1109/MetaMaterials.2015.7342513

[20] Zivieri R, Malagò P, Giovannini L: Band structure of collective modes and effective properties of binary magnonic crystals. Photon. Nanostruct. Fundam. Appl. 2014; 12: 398–418. DOI: 10.1016/j.photonics.2014.04.001

[21] Gubbiotti G, Malagò P, Fin S, Tacchi S, Giovannini L, Bisero D, Madami M, Carlotti G, Ding J, Adeyeye AO, Zivieri R: Magnetic normal modes of bicomponent permalloy/cobalt structures in the parallel and antiparallel ground state. Phys. Rev. B 2014; 90: 024419. DOI: 10.1103/PhysRevB.90.024419

[22] Krawczyk M, Puszkarski H: Plane-wave theory of three-dimensional magnonic crystals. Phys. Rev. B 2008; 77: 054437. DOI: 10.1103/PhysRevB.77.054437

[23] Donahue M, Porter D (Eds): OOMMF User's Guide Version 1.0. In: Interagency Report NISTIR 6376, National Institute of Standards and Technology, Gaithersburg, MD, 1999.

[24] Zivieri R. Metamaterial description of magnonic modes along ΓM direction in a 2D antidot lattice. In: Proceedings of the 7th International Congress on Advanced Electromagnetic Materials and Optics (Metamaterials' 2013); 16–21 September 2016; Bordeaux. 2013. pp. 181–183. DOI: 10.1109/MetaMaterials.2013.6808993 04/04/2016 http://ieeexplore.ieee.org/xpl/articleDetails.jsp?arnumber=6808993

[25] Buess M, Höllinger R, Haug T, Perzlmaier K, Krey U, Pescia D, Scheinfein MR, Weiss D, Back CH: Fourier transform imaging of spin vortex eigenmodes. Phys. Rev. Lett. 2004; 93: 077207. DOI: 10.1103/PhysRevLett.93.077207

[26] Kruglyak VV, Keatly PS, Neudert A, Hicken RJ, Childress JR, Katine JA: Imaging collective magnonic modes in a 2D arrays of magnetic nanoelements. Phys. Rev. Lett. 2010; 104: 027201. DOI: 10.1103/PhysRevLett.104.027201

IntechOpen